G-Functions for Multiple Interacting Pile Heat Exchangers

Revision date:	15 October 2013
Words in main text:	6387
No figures	11
No tables	6

First author		Fleur Loveridge[a]
Second author		William Powrie[b]
	a	Lecturer in Geomechanics Faculty of Engineering & Environment, University of Southampton
	b	Professor of Geotechnical Engineering and Dean of the Faculty Faculty of Engineering & Environment, University of Southampton
Corresponding author		Fleur Loveridge Faculty of Engineering & Environment Highfield, Southampton, UK, SO17 1BJ Fleur.Loveridge@soton.ac.uk 0044 (0)7773346203

G-Functions for Multiple Interacting Pile Heat Exchangers

Abstract

Pile heat exchangers – where heat transfer pipes are cast into the building piled foundations – offer an opportunity to use ground energy systems without the additional construction costs related to the provision of special purpose heat exchangers. However, analysis methods for pile heat exchangers are still under development. In particular there is an absence of available methods and guidance for the amount of thermal interaction that may occur between adjacent pile heat exchangers and the corresponding reduction in available energy that this will cause. This is of particular importance as the locations of foundation piles are controlled by the structural demands of the building and cannot be optimised with respect to the thermal analysis. This paper presents a method for deriving G-functions for use with multiple pile heat exchangers. Example functions illustrate the primary importance of pile spacing in controlling available energy, followed by the number of piles within any given arrangement. Significantly it was found that the internal thermal behaviour of a pile is not influenced appreciably by adjacent piles. (170 words)

Keywords: ground heat exchanger, pile, ground energy system, ground source heat pump system

Notation

AR	aspect ratio
B	pile spacing
c	concrete cover
G_c	concrete G-function
G_g	pile G-function
Fo	Fourier number or normalised time
H	pile length
$\dot{m}_{hp}$	mass flow rate of fluid at the heat pump
n	number of piles
Q	power
q	power per metre depth
S_c	specific heat capacity
S_{cv}	volumetric heat capacity
R_c	concrete thermal resistance
R_p	pipe thermal resistance
r_b	heat exchanger radius
T_b	temperature at pile-ground interface
T_f	mean fluid temperature
$T_{hp\text{-}in}$	temperature of fluid entering heat pump
$T_{hp\text{-}out}$	temperature of fluid leaving heat pump
$T_{i\text{-}in}$	temperature of fluid entering an individual pile
$T_{i\text{-}out}$	temperature of fluid leaving an individual pile
T_p	temperature at pipes
t	elapsed time

α_g	thermal diffusivity of ground
Φ	normalised temperature change
λ_c	thermal conductivity of concrete
λ_g	thermal conductivity of ground

1 Introduction

Installations of ground energy systems - where ground source heat pumps are connected to a series of ground heat exchangers to obtain sustainable heating and cooling - are increasing at a significant rate. Lund et al [1] report that the energy provided by such systems has more than doubled between 2005 and 2010. As the market has expanded, so has the range of types of heat exchanger used to provide the heat source. Traditionally, fields of borehole heat exchangers have been used to provide a large thermal capacity for major commercial or municipal buildings. However, where buildings require deep foundations it is becoming more common to make dual use of the piled foundations, equipping them with heat transfer pipes so that they can act as heat exchangers as well as structural components, eg [2] to [4]. This can lead to cost savings on projects by removing the need to construct special purpose heat exchangers.

Design methods for fields of borehole heat exchangers are well developed. Numerous different commercial software packages are available, some of which will be mentioned below. Typically these methods are also applied for the design of pile heat exchangers. However, there are important differences between borehole and pile heat exchangers which mean that application of borehole methods will underestimate the energy available from piles [5]. Heat transfer problems are typically controlled by their geometry and the thermal properties of the materials. The thermal properties of the materials for borehole and concrete pile construction are in a similar range, but their geometries are not. Piles have a much smaller aspect ratio (AR = heat exchanger length / diameter) than boreholes, which affects their long term thermal characteristics [5][6]. In addition, the larger diameter of piles results in a different short term behaviour with a greater proportion of short term energy storage happening within the heat exchanger itself, rather than just in the ground [5].

Previous work on pile heat exchanger design has focused mainly on determining the temperature changes with time, usually expressed as temperature response functions or G-functions, for a single pile [5], [7], [8]. However, all ground energy systems using pile heat exchangers will comprise multiple heat exchangers which will interact. With the exception of the Duct Storage Model [9] (which will be discussed below) no other specific solution for interacting pile heat exchangers has been published. This paper builds on previous work [5] and presents G-functions for multiple pile heat exchangers in some simple configurations, together with an approach for determining G-functions for any arrangement of piles. The impact on the available energy of different pile arrangements and spacings will be discussed, along with strategies for maximising the energy output.

2 Background

2.1 Design of Single Heat Exchangers

G-functions describe the change in temperature in the ground around a heat exchanger with time as the result of an applied thermal load. Usually both time and temperature change are normalised. Other normalisations are used, but this paper applies the following expressions, based on precedent from other studies, eg [7], [10]. The temperature change (ΔT) is normalised by the applied thermal load q (in W/m) and the thermal conductivity of the ground λ_g (in W/mK) such that:

$$\Phi \quad = \frac{2\pi\lambda_g}{q}\Delta T \qquad (\mathbf{1})$$

The elapsed time (t) is normalised by the ground thermal diffusivity (α_g) and the heat exchanger radius (r_b):

$$Fo = \frac{\alpha_g t}{r_b^2} \qquad (\mathbf{2})$$

Eskilson [11] pioneered the G-function concept. He assumed that ground heat exchangers act like a finite line heat source, operating within a uniform medium with an initial temperature equal to the far field boundary conditions and also the surface boundary condition. As a result of the constant temperature surface boundary condition the temperature response (Φ) will reach steady state at large values of time as the heat output is matched by that available. The time at which this occurs and the equilibrium temperature change depends on the aspect ratio of the heat exchanger. Eskilson's G-functions, published for AR=1000, were developed by means of a combination of analytical and numerical methods and form the basis of many commercial software packages.

Another commonly adopted approach is the cylindrical heat source [12], [13]. This is identical to the line heat source in the longer term, but accounts for the finite radius of the heat exchanger in the short term. This approach has been applied to the design of pile heat exchangers due to their larger diameter, but it has recently been shown [14] that the either the line heat source approach or the solid cylinder approach is more appropriate. While the classic cylindrical heat source assumes that the heat source is hollow, the solid cylinder model [8] assumes that heat may also flow into the centre of the heat exchanger. This makes it much more suitable for simulating pile heat exchangers.

All the above approaches take no account of the arrangement of heat transfer pipes within the pile cross section. Only two approaches overcome this limitation. Li & Lai [7] published G-functions based on the superposition of multiple line heat sources, with each line source representing a single pipe. This can produce theoretically accurate G-functions, but has the disadvantage of requiring a complicated calculation process for each specific pile diameter and pipe arrangement. This will be a barrier to its adoption on a routine basis. Loveridge & Powrie [5] presented upper and lower bound pile G-functions based on numerical analysis of a range of commonly constructed pile geometries (**Figure 1**). This removes the need to make new analytical solutions for every geometry but there is a trade-off in terms of a small reduction in accuracy.

Traditionally G-functions, describing the temperature change within the ground, are combined with a steady state resistance which determines the temperature change between the heat transfer fluid and the ground. However, recent work [15] has shown that this approach is conservative for pile heat exchangers and that greater energy efficiency can be obtained by taking a transient approach to the temperature change within the heat exchanger. Consequently Loveridge & Powrie [5] also proposed concrete G-functions which described the proportion of the steady state pile resistance which is appropriate for different values of normalised time, Fo.

Figure 1 Upper bound (left) and lower bound (right) pile geometries and material properties, assumes pipe diameter of 25mm

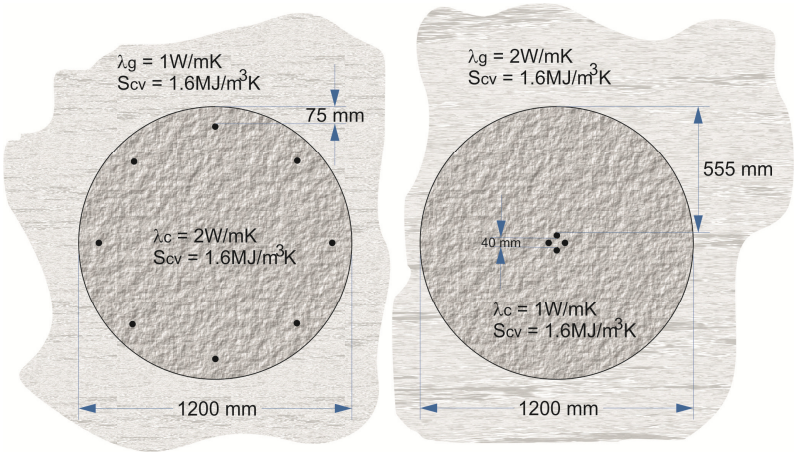

2.2 Multiple Heat Exchangers

If ground heat exchangers are positioned within a certain proximity of each other they will interact thermally to an increasing degree as time passes. If not accounted for in design, this will reduce the sustainability of a ground energy system over time. All multiple heat exchanger G-functions are based on the principle of spatial superposition. Eskilson [11] developed G-functions for many different arrangements of borehole heat exchangers. Software packages, such as Earth Energy Design (EED)[16] and GLHEPRO [17] are based on these, and typically use interpolation to cater for borehole arrangements different from those given in [11]. However, in all cases Eskilson's published G-functions are limited to the case where AR=1000 and are therefore not suitable for use with pile heat exchangers which typically have AR<50 [6]. In addition, Hellstrom et al [16] have shown EED to be unreliable for short heat exchangers (<15m); this effect has also been observed by Wood et al [18], [19]. The proprietary software ORPHEUS builds on GLHEPRO and overcomes some of the limitations by carrying out direct superposition for each specific arrangement of heat exchangers as requried, removing the need to interpolate between published G-functions. It also claims to be more applicable to piles of larger diameter, but further details are not given [20]. Similar superposition approaches can be taken with cylindrical source models, eg [21], [22] or equally any other single heat exchanger G-functions.

An alternative approach to G-functions for multiple heat exchangers is the so called Duct Storage Model or DST [9], [23], [24]. This assumes that a large number of vertical heat exchangers are installed close together to act as an underground thermal store. For local heat transfer around each pile or borehole an infinite line heat source is assumed for short duration heat pulses. Globally and at later times (defined as when the heat exchangers are thermally interacting) a steady state is assumed within the store and subsequent heat input leads to linear changes in temperatures throughout the store. The DST was initially validated against field data for small diameter (<50mm) borehole thermal stores in Sweden [25]. Subsequently, the DST approach has been implemented specifically for use with pile heat exchangers in the software PILESIM [26]. PILESIM has been validated against field data [27], focusing on the overall heat exchange capacity of the system. Independent analysis using time-stepping finite element models [28] implies that for regular arrays of piles the results provided by PILESIM are appropriate. However, the DST assumes a large number of identical piles installed in a regular array within a circular plan area and it is not clear what errors

result from smaller or less regular pile group arrangements that are more representative of typical foundation layouts. As with line and cylinder source based methods, the DST also assumes that the pile itself is at an instantaneous steady state, employing constant resistance values to account for the temperature difference between the fluid and the ground.

Numerical methods have also been used to assess multiple ground heat exchangers, eg [29], [30]; this has the advantage of being able to assess bespoke geometries and arrangements of heat exchangers. However three dimensional models of many heat exchangers can be computationally expensive and hence 2D simplifications may be preferable. This, however, has the disadvantage of not being applicable to long term conditions. One 2D model has been used to test the applicability of using regular arrays of heat exchangers as a simplified representation of irregular arrangements. This is particularly relevant for pile heat exchangers as the pile positions are governed by the structural layout of the building and not usually installed on a grid pattern. Teza et al [31] concluded irregular patterns can be replaced by regular ones for analysis with a temperature prediction accuracy of of ± 1°C, provided that the average spacing and plan area are equivalent between the two cases.

2.3 Heat Exchanger Configuration

The heat transfer pipes from multiple heat exchangers can be connected in series, in parallel or in a combination of both. This detail has an impact on the temperatures that develop around each individual heat exchanger. For pile heat exchangers connected in parallel the inlet temperature to each pile ($T_{i\text{-}in}$) will be equal to the outlet temperature from the heat pump ($T_{hp\text{-}out}$). If all n piles in the system are of the same geometry then each pile will also be subject to the same flow rate ($\dot{m}_{hp}/n$), and assuming that the heat transfer to each is also equal, the return temperature to the heat pump ($T_{hp\text{-}in}$) will be equal to average outlet temperature ($T_{i\text{-}out}$) from all of the piles:

$$T_{hp-in} = \frac{\sum_1^n T_{i-out}}{n} \qquad (3)$$

If the design is based on a specified total thermal input $Q = nHq$ (in W), then for n piles of length H, it is also true that:

$$Q = S_c \dot{m}_{hp}\left(T_{hp-in} - T_{hp-out}\right) \qquad (4)$$

where S_c is the specific heat capacity (J/kgK) and $\dot{m}_{hp}$ is the mass flow rate (kg/s) of the heat transfer fluid at the heat pump. The G-function for the multiple heat exchangers, calculated by superposition, is used to determine the mean fluid temperature for the heat exchangers, T_f, where:

$$T_f = \frac{\sum_1^n (T_{i-out} + T_{i-in})}{2n} \qquad (5)$$

The inlet and outlet temperatures to the heat pump can then be determined as follows (where positive thermal loads represent heat injection to the ground):

$$T_{hp-out} = T_f + {}^{Q}\!/_{2S_c \dot{m}_{hp}} \qquad (6)$$

$$T_{hp-in} = T_f - {}^{Q}\!/_{2S_c \dot{m}_{hp}} \qquad (7)$$

This calculation clearly depends on the important assumption that the heat flux q to each pile is the same. Eskilson suggests that this simplification is valid for heat exchangers in parallel, with discrepancies to more detailed calculations being of the order of 0.1°C [11]. He also suggests that the error would be larger if the heat exchangers are coupled in series or if there is a variation of q along their length, although the size of this error is not specified.

If the piles are connected in series then all piles will be subject to the same fluid flow rate as the heat pump. The inlet temperature to each pile will always be equal to the outlet temperature of the preceding pile in the circuit. Both the temperature difference between pile inlet and outlet and the heat flux to each pile will now be different. The length of the series circuit of piles will determine how big the errors are when using **Equations 3** to **7** above. In reality most systems consist of a combination of series and parallel circuits to optimise the flow conditions. Calculation of the exact inlet and outlet temperature to each individual pile is therefore very time consuming. Fortunately Katsura et al [22] have shown that simplifications, including assuming each series circuit acts as one heat exchanger, provide sufficiently accurate results. Providing the piles are all the same geometry, this is effectively the same as assuming all individual heat exchangers operate in parallel. While more complicated approaches can be adopted, and it has been shown that maximum energy output can be obtained by adjusting the flow rate and position of each pile individually [32], [33], this complexity is considered beyond the scope of the current paper. Instead we focus on providing the first multiple heat exchanger G-functions specifically for pile heat exchangers and investigating how typical piled foundation arrangements can affect energy efficiency.

3 Multiple Pile G-Functions: Ground Temperature Response

3.1 Two Pile G-Functions

Single pile G-functions have been presented by the authors in [5]. These were derived by numerical analysis methods, using two dimensional cross sections through the pile for short timescales to determine lower and upper bound conditions and larger three dimensional models to take into account the development of a steady state in the longer term. The geometry and material properties for the upper and lower bound piles are shown in **Figure 1**. Generally large diameter piles with pipes installed close to the pile edge are represented by the upper bound, while large diameter piles with pipes installed in the centre of the pile are represented by the lower bound. Smaller diameter piles and those with pipes installed in intermediate positions fall between the bounds. In addition, piles where the concrete thermal conductivity (λ_c) is greater than that of the ground (λ_g) tend towards the upper bound, while the reverse conditions $\lambda_g > \lambda_c$ tend towards the lower bound.

3.1.1 Basis

For Fo<200 The 3D model used to develop the single pile G-functions was applied to determine revised functions for two piles interacting. Full details of the model development and validation are given in [5]; summary characteristics are given in **Table 1**. For Fo>200 finite line source methods are applicable. In this case the finite line source was evaluated numerically on the basis on an axisymmetric model constructed in ABAQUS. This allowed any pile spacing to be easily assessed.

The heating input was applied at the position of the pile radius as shown in **Figure 2**. Although this effectively makes the model a finite cylinder, this is equivalent to a line source after a short time period and the model output was used only for Fo>200. Full details of the model are given in [14] with summary characteristics provided in **Table 2**.

Figure 2 Schematic of axi-symmetric finite line source model

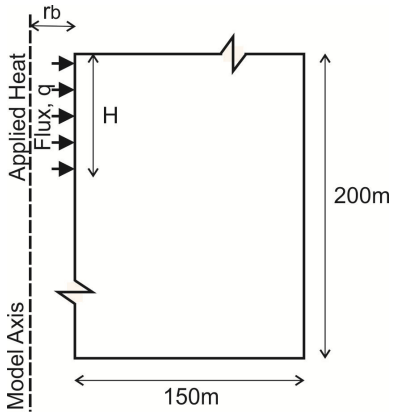

To calculate the G-function for two piles interacting the temperature change at $r=r_b$ at the edge of a single pile was added to the temperature change in the model at r=B where B is the centre to centre spacing between the two piles. As the pile arrangement is symmetrical and both piles suffer the same degree of interaction then the G-function only needs to be calculated for one pile. The length of both piles is then taken into account when determining the applied heat flux as $q = Q/2H$.
When presenting his G-functions, Eskilson normalised the heat exchanger spacing B by the length of the heat exchanger, H [11]. However, with piles we have found it more practical to normalise by the pile diameter $2r_b$, as a result of existing practice in the piling industry. First, pile spacings are often specified as a centre to centre spacing in terms of a multiple of the diameter. Secondly, pile lengths are often determined by geological features, such as the presence of a hard stratum or the need to avoid penetrating into an underlying aquifer. In addition, while Eskilson only published G-functions for AR=1000, it is important to consider a range of smaller ARs for piles. Values of 15, 25, $33^1/_3$ and 50 have been used on the basis of a survey of constructed geometries [6].

3.1.2 Results

Two-pile G-functions for the extreme cases of AR=15 and AR=50 are plotted in **Figure 3** for different $B/2r_b$ values from 1.2 (the closest piles are typically spaced) to 20 (where the influence of adjacent piles diminishes). The influence of the pile spacing is clear, with much greater temperature changes at steady state for those piles at closest spacing. **Table 3** gives an indication of the maximum interaction experienced by the piles, measured as a percentage increase in Φ in the long term. This clearly shows the greater interaction for higher AR piles, but also the important influence of the spacing between the piles. For $B/2r_b = 20$, increase in Φ values are always less than 15%. However, for $B/2r_b = 1.2$, Φ increases by up to 76%. These increases in Φ mean that there are diminishing returns available from multiple piles as their spacing decreases. This means that for the closest spacing, less than 60% of the energy that could be obtained from a single pile is available from each of the pair of piles. Therefore in total 1.2q is available compared with 2q for two isolated piles. This means significantly diminishing returns as piles get closer together.

Figure 3 and **Table 3** also show that the higher aspect ratios have greater values of Φ as a steady state develops, and also a greater degree of interaction as seen by the bigger increase in Φ and corresponding reduction in equivalent energy for the two pile case. Piles with a lower aspect ratio interact to a lesser extent due to the earlier and more significant influence of the surface boundary condition. This restricts both the overall temperature change that can occur, and also the distance to which temperatures within the ground are influenced by the heat exchanger. This suggests that low aspect ratio piles have the potential to be more efficient due to i) reduced temperature changes in the ground and ii) reduced interactions between adjacent heat exchangers.

Table 1 Main characteristics of 3D pile G-function model, see also [5]

Pile geometry	As Figure 1, but with AR = 15, 25, $33^1/_3$, 50
Model extent	To a distance of 25m radially and below the pile; quarter pile modelled for computational efficiency
Heat transfer	By conduction only; pipes and fluid not modelled as these reach a steady state rapidly
Initial conditions	Constant temperature (T = 0^oC) applied throughout
Boundary conditions	Constant heat flux applied at pipe outer radius Constant temperature (T = 0^oC) applied at far field boundaries and ground surface Insulated boundaries on the planes of symmetry
Elements	8 node linear heat transfer brick elements
Mesh sizes	5 mm at pipes; 10 mm at pile edge; 2.5 m at far field; 0.5 m along pile length
Material properties	Refer to Figure 1
Validity	Fo ≤ 200
Software used	ABAQUS 6.10-2

Table 2 Main characteristics of axis-symmetric finite line source model, see also [14]

Pile geometry	As Figure 2, with r_b=0.6m and AR = 15, 25, 331/3, 50
Model extent	To a radial distance of 150m and depth of 200m
Heat transfer	By conduction only; pile not modelled as applied in long term only
Initial conditions	Constant temperature (T = 0^oC) applied throughout
Boundary conditions	Constant heat flux applied at pile radius over the full length of the pile, insulated below the pile toe. Constant temperature (T = 0^oC) applied at far field boundaries and ground surface
Elements	4-node linear axisymmetric heat transfer quadrilateral elements
Mesh sizes	10 mm at pile edge; 5 m at far field; 1 m along pile length
Material properties	As Figure 1
Validity	Fo > 200
Software used	ABAQUS 6.10-2

Table 3 Steady state increase in Φ and equivalent energy output for a pair of piles for different spacings and aspect ratios (AR)

$B/2r_b$	AR=15 Increase in Φ	AR=33 Increase in Φ	AR=25 Increase in Φ	AR=50 Increase in Φ
20	3%	6%	8%	12%
10	9%	15%	19%	25%
5	23%	30%	34%	40%
3	37%	44%	48%	52%
2	49%	56%	59%	63%
1.5	59%	65%	67%	70%
1.2	67%	71%	74%	76%

Note: equivalent energy is the energy available at steady state per pile compared to the single pile case.

Figure 3 Pile G-functions for two piles interacting at different $B/2r_b$ values: a) AR=15 Lower Bound; b) AR=15 Upper Bound; c) AR=50 Lower Bound; d) AR=50 Upper Bound. In each case the curves are, from top to bottom, $B/2r_b$ = 1.2, 1.5, 2, 3, 5, 10, 20 and ∞ respectively.

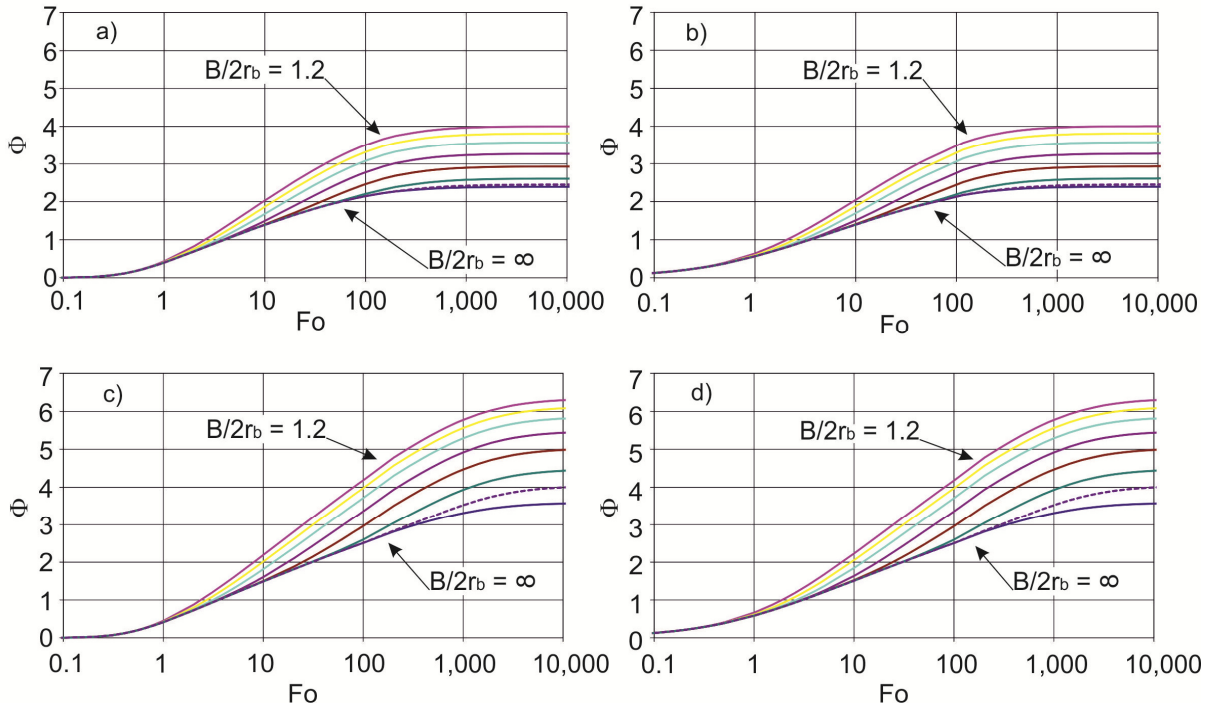

Figure 4 plots Φ vs Fo for different aspect ratios, showing that the upper and lower bound cases experience identical interaction in the long term for a given aspect ratio. However, the short term there is a small increase in interaction for the upper bound case. This is to be expected given the greater proximity of the pipes to the pile edge. Overall **Figure 4** shows that the interactions are similar at small values of time regardless of the pile spacing and pile geometry. This is also to be expected as the zone of steep temperature gradients has yet to reach far beyond the pile. However, as time increases larger aspect ratio piles interact more and for longer.

Eskilson reported that there is no interference between borehole heat exchangers if B>H and that any interactions are small as long as B>H/2 [11]. For the case of pile heat exchangers, the latter criterion is equivalent to $B/2r_b>AR$. Reference to **Figure 4** shows that these guidelines remain true for pile heat exchangers and that in this case "small interactions" are approximately equivalent to a 5% increase in Φ. However, for pile heat exchanger systems, where the pile layout and spacing is governed by the structural and geotechnical design of the building and foundations, it would be exceedingly unlikely for the spacing the piles to be 15m or more. Therefore in most cases some interactions will occur.

Figure 4 Percentage increase in Φ for different normalised pile spacings and aspect ratios (AR): a) AR=15; b) AR=25; c) AR=33; d) AR=50. Solid lines for upper bound cases; dashed lines for lower bound cases.

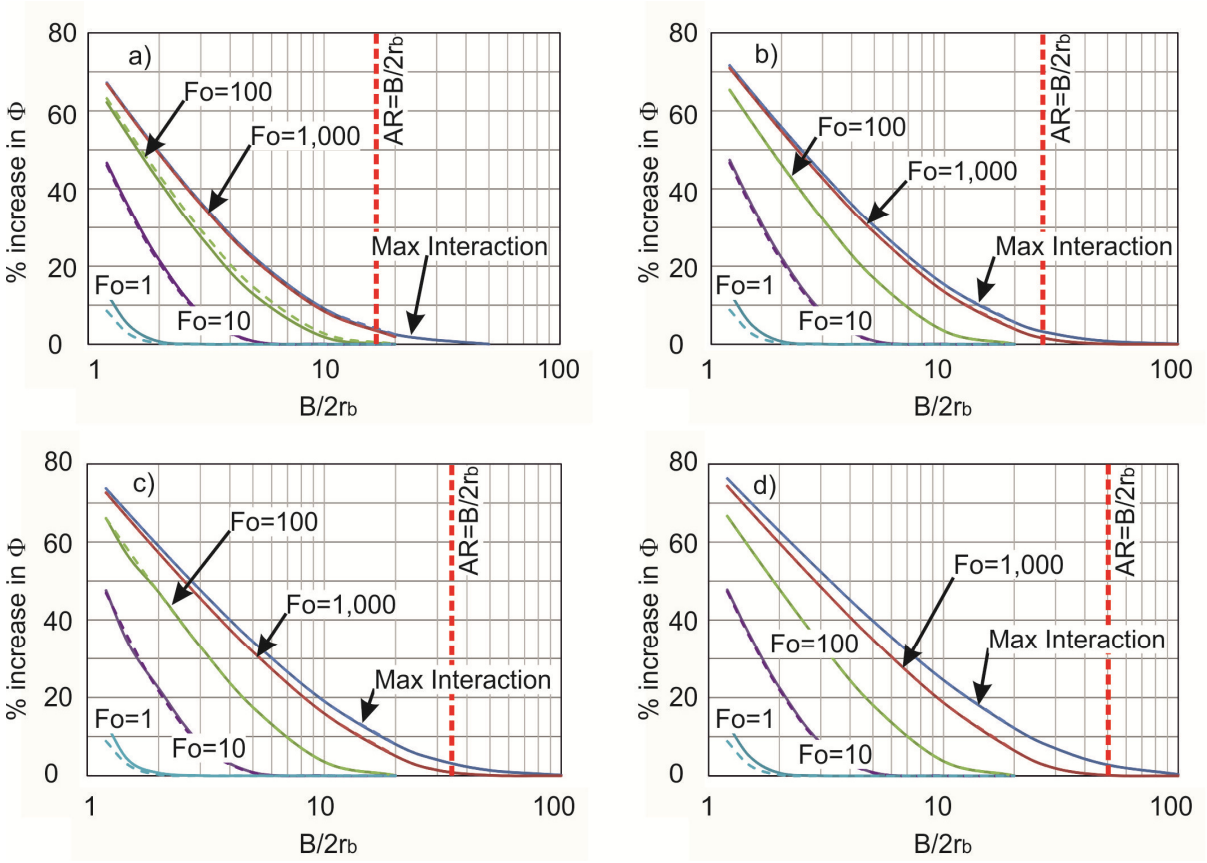

3.2 Multiple Pile G-functions

Using **Figures 3** and **4** and **Table 3** it is possible to interpolate the influence of piles at any spacing and hence compile the average multiple pile G-function for any arrangement of piles. For brevity, two examples are included below; three piles in a line (**Figure 5**), which may be an arrangement beneath a building column and 9 piles in a grid (**Figure 6**), which gives an idea of the degree of influence of many pile heat exchangers. In reality most pile arrangements are irregular and related to the structural layout of the building, in particular under the positions of the columns that transfer most of the vertical load to the foundations. A column may be supported by two or three closely

spaced piles, with many columns being present at larger spacings. However, the following method may be used for any arrangement.

It has been assumed, for the purpose of the examples, that the pipes are installed near the edge of the pile and therefore an upper bound pile G-fucntion has been used. An aspect ratio of 50 has been chosen because this provides an upper estimate to the likely interactions for pile heat exchangers. Curve fitting was then applied to **Figure 4d** so that the percentage increase in Φ for any pile spacing would be determined. For three piles in a line (**Figure 5**) the G-function will then be equal to the average response of the three piles, one of which will suffer interactions from two of its neighbours at spacing B and two of which experience interactions from two piles at B and 2B spacing respectively. The same procedure can be applied for the nine pile arrangement (**Figure 6**), except here there are 4 corner piles, 4 centre edge piles and one central pile, all of which have different combinations of interactions which must be averaged.

Figure 5 G-function for three upper bound piles in a line, with AR=50. From top to bottom $B/2r_b$ = 1.2; 1.5; 2; 3; 5; 10; 20; ∞.

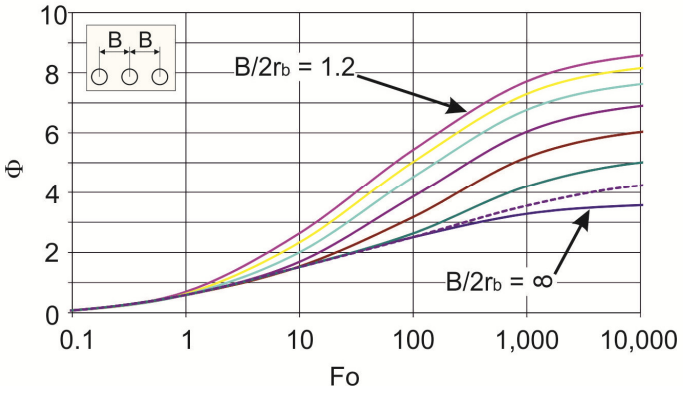

Figure 6 G-function for nine upper bound piles arranged on a grid, with AR=50. From top to bottom $B/2r_b$ = 1.2; 1.5; 2; 3; 5; 10; 20; ∞.

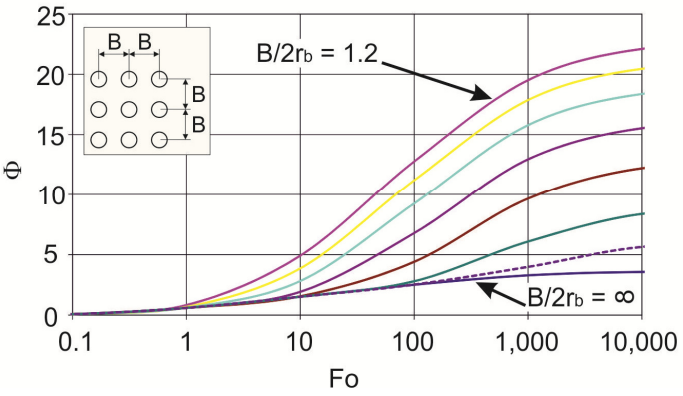

Figures 5 and **6** show the significant impact that multiple pile heat exchangers can have when interacting. For a single pile (B=infinity) with AR=50, the long term steady state normalised temperature response (Φ) is approximately 3.6. For two piles at $B/2r_b$=1.2 the response increases to 6.3, for three piles and nine piles at the same spacing it is 8.6 and 22.2 respectively. These are large increases and will result in a corresponding decrease in the energy that can be exchanged per linear

metre of the pile. **Table 4** summarises the increase in Φ for the closest spacing. These increases mean that at steady state with nine piles in a grid that each pile is only delivering 16% of the energy of an individual isolated pile. However, it is rare for so many piles to be spaced so closely and in reality combination arrangements above as described above are more common. In addition, this analysis has assumed that all of the nine piles are equipped as heat exchangers. The results show that while each additional pile used as a heat exchanger does increase the overall quantity of energy available there are diminishing returns. When the energy required for fluid circulation is also taken into account it may be more economical to equip only some of these piles with heat transfer pipes.

Table 4 Steady state increase in Φ and equivalent energy output for different pile arrangements compared to a single pile (AR=50)

No piles	**Spacing**	**Increase in Φ**
Single pile	N/A	N/A
2 piles	$B/2r_b$=1.2	76%
3 piles in a line	$B/2r_b$=1.2	141%
9 piles in a grid	$B/2r_b$=1.2	521%

4 Multiple Concrete G-functions: Internal Pile Temperature Response

The multiple pile G-functions presented in Section 3 describe the average temperature change with time in the ground around the heat exchangers. However, it is important to determine whether the nature of the temperature changes within the pile are also affected by the interaction of the heat exchangers. To our knowledge this has not been ascertained before. Previously the authors have presented concrete G-functions to describe the transient behaviour of the pile concrete [5]. This is an improvement on the previous approach of assuming the pile concrete is at steady state. The first concern for multiple piles is whether the change in temperature field for two or more piles will influence the steady state value of the pile thermal resistance. Secondly, we need to understand whether the shape of the concrete G-function, expressed as a proportion of the steady state R_b with time, changes when there are more than one pile in proximity.

To answer these questions, the numerical model used in [5] was extended to represent two piles, taking advantage of a line of symmetry between the piles to minimise the computational effort required (**Figure 7**). Full details of the model set up and validation are given in [5] and [14], with updated geometry and a summary of the conditions analysed provided in **Table 5**. Only the upper and lower bound pile concrete conditions, as identified in [5] and given in **Table 6**, were analysed. These include upper and lower bounds for the two cases of pipes installed centrally and those closer to the pile edge. As the lower bound piles are 300mm in diameter with two pipes installed, it is necessary to compare two cases. Case #1 is where the two pipes are aligned perpendicular to the line of symmetry in the model (as shown in **Figure 7**) and Case #2 is where the pipes are aligned parallel to the line of symmetry. It should also be noted that lower and upper bound cases used for the concrete G-function are different from the lower and upper bound cases used for the pile G-functions as they relate to the behaviour of the concrete not of the ground.

Figure 7 Schematic of numerical model for 2D analysis of concrete resistance and temperature response (showing Case #1, not to scale). Refer also to Table 5.

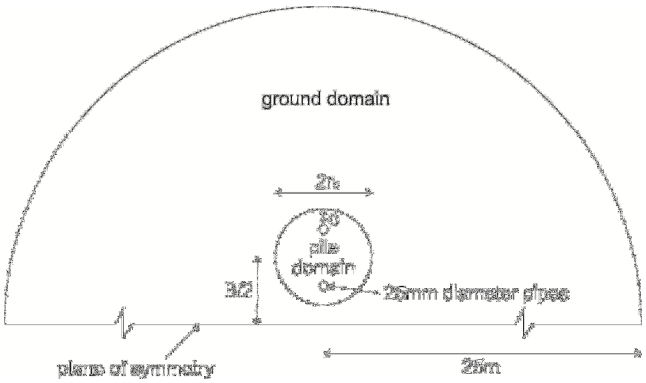

Table 5 Main characteristics of 2D concrete G-function model, see also [5],[14]

Pile geometry	Upper and lower bound pile geometries as per Table 6
Model extent	To a distance of 25m from the model centre (Figure 7)
Heat transfer	By conduction only; pipes and fluid not modelled as these reach a steady state rapidly
Initial conditions	Constant temperature (T=0^{o}C) applied throughout
Boundary conditions	Constant heat flux applied at pipe outer radius Constant temperature (T=0^{o}C) applied at model edge Insulated boundary at plane of symmetry
Elements	Triangular
Mesh sizes	2mm at pipes; 10mm at pile edge; 0.5m model edge
Material properties	Refer to Table 6
Validity	Fo ≤ 10
Software used	COMSOL 4.3

Table 6 Steady state thermal resistance (R_c) for individual and pairs of interacting piles

		Lower Bound 300mm diameter pile, 2 pipes λ_c=1; λ_g=2	**Upper Bound** 1200mm diameter pile, 4 central pipes or 8 near edge λ_c=2; λ_g=1
Central Pipes; c=105mm for $2r_b$=300mm; c=555m for $2r_b$=1200mm.	Single Pile	0.267 mK/W	0.231 mK/W
	Two Piles #1	0.267 mK/W	0.231 mK/W
	Two Piles #2	0.267 mK/W	N/A
Pipes Near Edge; c=50mm for $2r_b$=300mm; c=75m for $2r_b$=1200mm.	Single Pile	0.183 mK/W	0.029 mK/W
	Two Piles #1	0.187 mK/W	0.029 mK/W
	Two Piles #2	0.180 mK/W	N/A

4.1 Steady State Resistance for Two Interacting Piles

At any given time the thermal resistance of the concrete part of the pile is calculated as follows:

$$R_c = \frac{\overline{T_p} - \overline{T_b}}{q} \qquad (8)$$

where $\overline{T_p}$ and $\overline{T_b}$ are the integral mean values of the temperature at the pipes and the pile edge boundaries respectively, and q is the total heat flux (in W/m) applied to the all the pipe boundaries. The steady state resistance is the asymptotic value R_c calculated at larger values of time, typically when Fo approaches 10. **Table 6** presents the steady state values of R_c for single and pairs of interacting piles. In most cases the presence of an additional pile has no noticeable impact on the steady state resistance, despite some changes to the heat flow paths that the additional pile must cause. The exception to this is the lower bound case with pipes near to the edge. Here the steady state resistance now depends on the relative arrangement of the two pipes in the adjacent piles. For Case #1 the resistance is increased by 2%, while for Case #2 it is decreased by 2%. These differences are not significant in the context of construction tolerances for the positioning of the pipes within the piles. In addition, the construction process will give limited control of the orientation of any pair of pipes, and therefore the final orientation will be almost random. Therefore, overall, it is considered appropriate to continue using the steady state resistance of a single pile regardless of the number and spacings of adjacent piles.

Figure 8 Concrete G-functions for individual and pairs of interacting piles: a) pipes placed centrally; b) pipes placed near the pile edge. Solid lines are for individual piles; short dashed lines are two piles Case #1; long dashed lines are two piles Case #2.

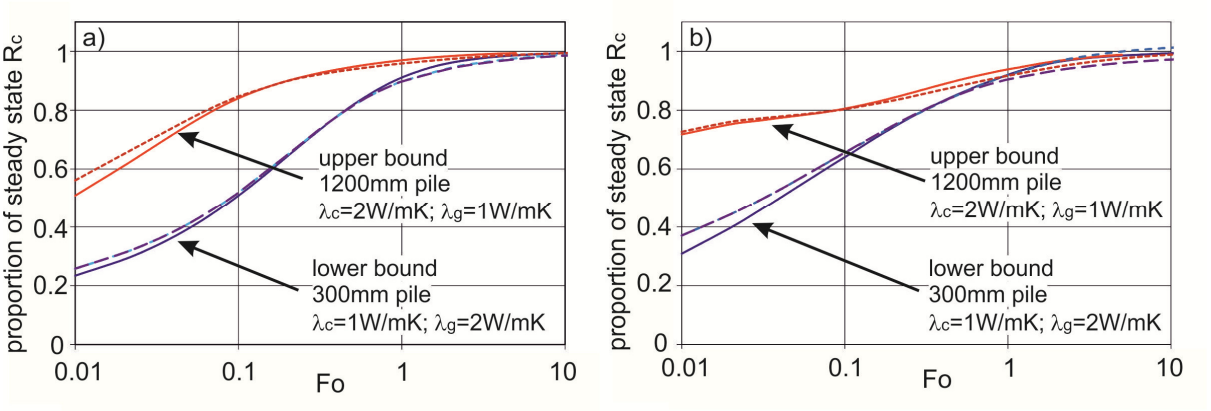

4.2 Concrete G-functions for Two Interacting Piles

The second question that needs to be answered is whether the shape of the concrete G-function curve, ie how the transient value of thermal resistance for the pile changes with time, is affected as a result of piles interacting**. Figure 8a** and **Figure 8b** plot concrete G-functions for upper and lower bound cases for the scenario of pipes placed centrally and near the edge respectively. In both cases the solid lines represent the G-function for a single pile and the dashed lines represent those for two piles interacting. There is some difference between these cases, but typically these are within a few percent. The exception is the lower bound case with pipes near the edge where the difference between the single and two pile scenarios is initially 20%, rapidly falling to around 2% by Fo=0.1.

Given that the lower bound represents smaller diameter piles and that Fo=0.1 is equivalent to less than one hour for a 300mm diameter pile, this difference is minor in the context of standard 1 hour time stepping used in design. Therefore, while it is possible to produce new concrete G-functions for the interacting cases in **Figure 8**, it will be sufficient in most scenarios to use the curves for single piles presented (with curve fit data) in [5].

5 Impact on Energy Storage

To illustrate the impact of interactions between multiple pile heat exchangers on the thermal energy that can be extracted from the ground, three cases have been compared using the multiple pile G-functions presented in Section 3:

- A single pile ($B/2r_b$ = infinity in **Figure 3d**),
- Two piles installed at a spacing of $B/2r_b = 1.2$ (**Figure 3d**),
- Nine piles installed on a grid pattern with $B/2r_b = 3$ (**Figure 6**).

In all cases AR=50 has been assumed as this represents the worst case interactions. The piles have been selected to be 450 mm diameter and 22.5 m long with a concrete thermal conductivity of λ_c=1 W/mK. The surrounding ground is assumed to have thermal properties λ_g=2W/mK and α_g=1x10^{-6} m^2/s. The pile concrete thermal resistance R_c is 0.075 mK/W and the pipe resistance R_p is 0.025 mK/W for four pipes placed near the edge of the pile. Consequently an upper bound pile G function for AR=50 is used to describe the temperature change in the ground, while a lower bound concrete G-function for pipes placed near the edge is used to determine the temperature change within the pile. The following equation is used to calculate the mean temperature change in the heat transfer fluid:

$$\Delta T_f = qR_p + qR_c G_c + \frac{q}{2\pi\lambda_g} G_g \qquad (9)$$

where G_c is the concrete G-function and G_g is the pile G-function. As the applied thermal load q (in W/m) is not constant, but changes with each time step, superposition must be used with each G-function so that the change in temperature can be calculated:

$$\Delta T_n = \sum_{i=1}^{i=n} \frac{q_i}{2\pi\lambda_g} \left[G\left(Fo_n - Fo_{(i-1)}\right) - G\left(Fo_n - Fo_i\right) \right] \qquad (10)$$

where n is the point in normalised time in which the superposition is evaluated and G is the G-function (whichever one is being used in a particular case) calculated at the value of Fo prescribed in the equation. Equation 10 has been coded in the software Matlab to allow calculation of the sum in hourly timesteps for the period of one year.

For the examples being considered q is obtained from the building thermal load profile shown in **Figure 9**. The profile is given for a typical year and has been developed from a numerical simulation of a modern multi-use development in the South East of England, scaled down to an appropriate level for a single pile. The total demand is 1.72 MWhrs heating and 1.76 MWhrs cooling per pile. However, despite the overall energy demand being close to balanced, the peak power values for

cooling are much higher than those for heating, being comprised of shorter duration but greater magnitude power peaks. It will be seen that this has an impact on the resulting temperature changes.

Figure 9 Example thermal loads for one year commencing in January (insets shows daily cycle detail)

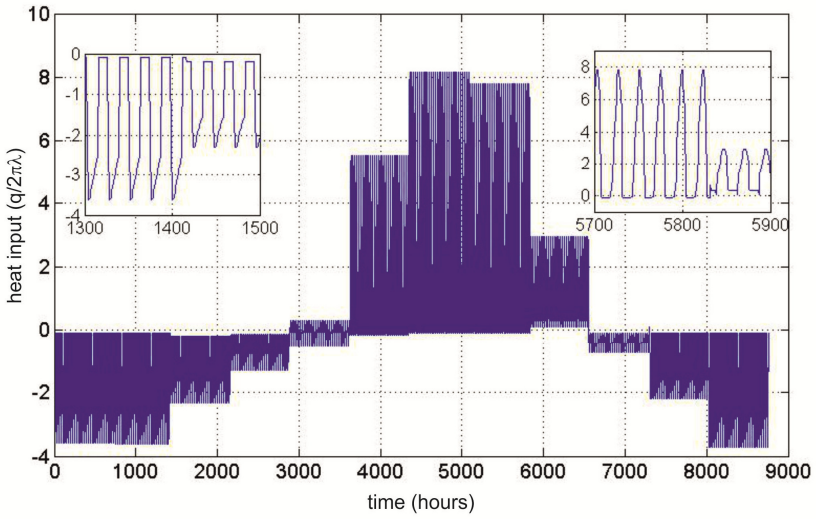

Note: positive thermal loads are heat injection to the ground (building cooling); negative thermal loads are heat extraction from the ground (building heating)

Figure 10 Calculated Mean Fluid Temperatures for Different Numbers and Arrangements of Piles

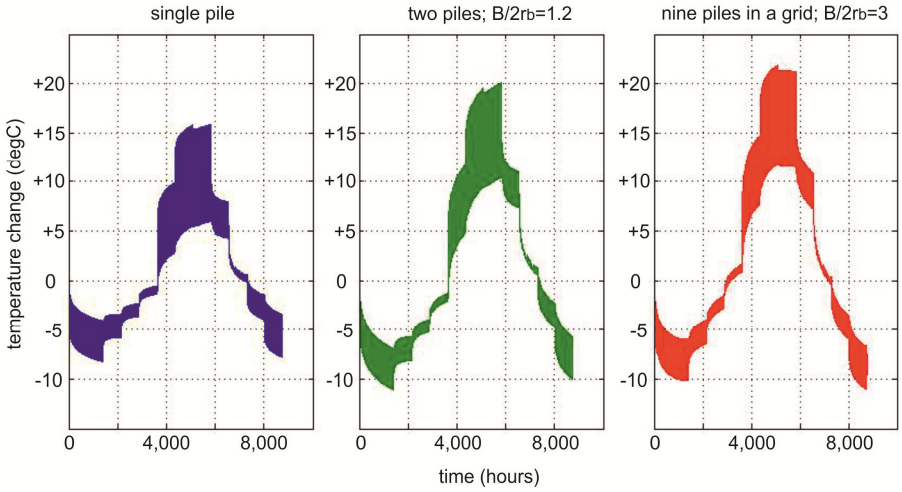

5.1 Results

The calculated mean fluid temperatures (T_f) are shown in **Figure 10**. The actual inlet and outlet temperatures to the heat pump would actually cover a wider range than this (as per Equations **6** and **7**). However, these values have not been calculated as they would depend on the mechanical design of the pipework for any particular system, which would need to be optimised to maintain a sensible temperature differences across the heat pump. **Figure 10** shows the calculated temperature changes for the first year, which range from -8.3°C to +15.9 °C for single pile to -11.1 °C to +20.1 °C for two piles at $B/2r_b$ = 1.2 and -11.0 °C to +21.8 °C for nine piles at $B/2r_b$=3. It is interesting to note that initially the two pile scenario has a greater temperature change that the nine pile scenario. This is

due to the closer spacing and the interaction effects commencing at a shorter time. In the longer term the temperature change for the nine pile arrangement is much greater, especially in the summer when the rate of change of thermal load is greatest. It is expected that the differences between the three cases would increase with time.

Assuming a typical initial ground temperature of 12°C it is reasonable to apply limits on the mean fluid temperature change of -10 °C and +20 °C (ie absolute limits of 2°C and 32°C). Then the average energy available per pile can be calculated using **Equation 9** assuming that ΔT_f remains within the range of these limits. As in [5], for simplicity, the shape of the thermal load profiles in **Figure 9** has not been changed, but the values of applied thermal load has been adjusted pro-rata to give an indication of the impact the interactions are having on the thermal capacity of the piles. In reality the system would be adjusted to cover as much base load as possible with some extreme peak loads being be supplied by an auxiliary system. The assessment would also cover the full design life of the structure rather than just the first year as is shown here.

Figure 11 shows the relationship between the average energy available per pile and the imposed temperature limits for the one year period analysed. Based on the -10°C temperature change limit the available average heating energy per pile is 2069 kWh, 1546 kWh and 1564 kWh for one pile, two pile and nine piles respectively. Interestingly the nine pile case is actually slightly greater than the 2 pile case. This is because the nine piles are at greater spacing and the analysis starts in the winter with heating. If the analyses were carried out over a longer time period, there would undoubtedly be less energy available for the nine pile case than for the 2 pile case. In terms of cooling, using the +20°C limit, the available average energy for each pile is 2219 kWh, 1746 kWh and 1611 kWh for one pile, two pile and nine piles respectively. The range of values is similar to the heating case, but as the cooling season comes later in the analysis period there is a greater difference between the two pile and nine pile cases. Despite the similar amounts of energy extracted in heating and cooling the temperature changes are bigger in cooling due to the higher peak loads. This illustrates the importance of understanding both the monthly and total energy demands of a systems and the shorter term variations in demand which will result in the peak loads.

Figure 11 Relationship between allowable fluid temperature change and available energy for example pile arrangements: a) heating; b) cooling

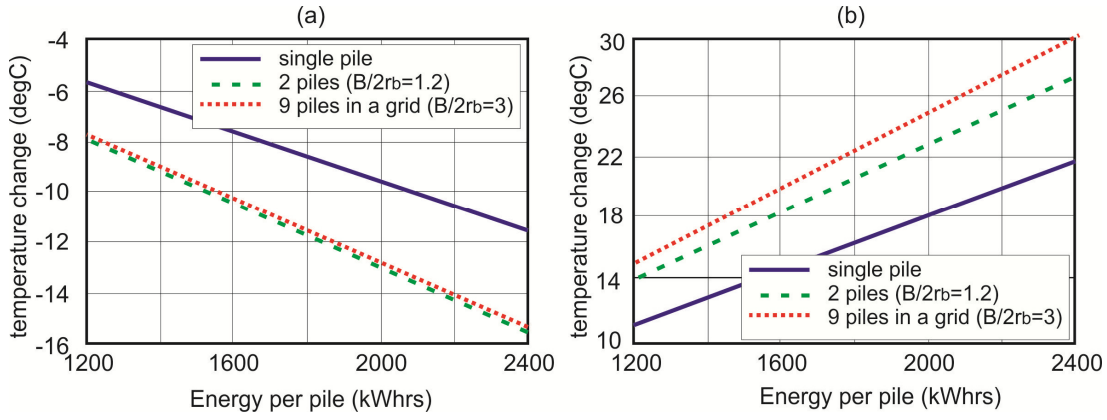

In total the average energy available per pile in the three arrangements is 4288 kWh, 3292 kWh and 3175 kWh for the single pile, two pile and nine piles cases respectively. This represents a 23% drop in available energy from one to two piles and a further 26% drop for the nine pile case. It is interesting

that these two figures are of the same order, despite a much larger number of piles in the nine pile case. This reflects the importance of pile spacing and the much reduced interactions when the pile spacing is opened from $B/2r_b$=1.2 to $B/2r_b$=3. The equivalent energy for the nine pile arrangement is 51% compared with 23% for that arrangement at steady state. This indicates that there is the potential for the efficiency of the system to decline further over the lifetime of the building. For the 450mm diameter piles analysed one year represents Fo=623. Steady state conditions (under constant thermal load) is in excess of Fo=10,000, or around 16 years.

6 Discussion

Ground heat exchangers installed in multiple piles will interact adversely in terms of energy available per pile, generally by less than 5% as long as $B/2r_b$>AR. However, given the cost of constructing deep foundations, priority will always be given to optimising pile layouts with respect to their structural function, that of supporting the overlying building. This means that it is not possible to adjust the positions of pile heat exchangers to increase the spacing and hence maximise the energy output. However, an assessment of the potential for interactions (increased temperature change or reduce energy output) between adjacent piles should still be carried out.

The example analyses presented have shown how the effect of adjacent piles can greatly reduce the energy output from each individual pile. Overall the total energy obtained from multiple piles is always greater than from a single pile, but as the number of piles is increased and the spacing reduced the energy return per pile decreases. In some extreme cases it may be more economical to equip only some piles in a foundation layout with heat exchange pipes. While the pipes themselves are of relatively low cost, there is additional programme time for installing the pipes and additional running costs for a longer pipe circuit. These would need to be weighed against the energy gains from the interacting piles.

The degree of interactions between adjacent pile heat exchangers will depend on a number of factors. The spacing of the piles is important, but so is the number of piles. The spacing will have the biggest impact on the time taken for interactions to become significant, while the number of piles in the arrangement (in combination with their spacing) will impact the long term energy obtainable. Generally smaller aspect ratio piles will interact to a lesser extent than larger aspect ratio piles, which means that the former can be successfully implemented at closer spacings. The nature of the thermal load is always important for the performance of ground heat exchangers and this case is no exception. Short term variations in load will reduce interactions compared with a sustained base load.

7 Conclusions

This paper presents a method for determining new G-functions for use in the thermal analysis of multiple interacting pile heat exchangers. Example pile G-functions, which describe the temperature change in the soil around a pile with time, are presented for a number of examples configurations. The key conclusions of this study are:

- If multiple adjacent piles are used as heat exchangers then there will be adverse thermal interactions between the heat exchangers. These interactions will become more significant

over the lifetime of the energy system, but will also be dependent on the nature of the thermal load. For example highly fluctuating thermal demands will reduce the potential for interactions between heat exchangers.

- Heat exchangers with smaller aspect ratios are affected less by thermal interactions. Thus interactions between piles will be less than those between traditional borehole heat exchangers installed at the same spacing, potentially leading to more energy efficient systems.
- However, as pile spacing is usually governed by the overlying structure, piles are generally more closely spaced than typical borehole arrangements.
- Consequently, it is not always advantageous to equip all piles within a pile group with heat transfer pipes.
- The degree of interactions to be expected for a given scheme can be calculated using the methods for multiple pile G-functions described in this paper.
- Significantly, it was found that the changes to the temperature field within concrete piles are not sufficient to cause appreciable changes to either the transient or steady state resistance of the pile.

References

[1] Lund, J. W., Freeston, D. H. & Boyd, T. L. (2011) Direct utilization of geothermal energy: 2010 worldwide review, Geothermics, 40(3), 159 – 180.

[2] Hamada, Y., Saitoh, H., Nakamura, M., Kubota, H. & Ochifuji, K. (2007) Field performance of na energy pile system for space heating, Energy and Buildings, 39, 517 – 524.

[3] Gao, J., Zhang, X., Liu, J. Li, K. & Yang, J. (2008) Thermal performance and ground temperature of vertical pile foundation heat exchangers: a case study, *Applied Thermal Engineering*, 28, 2295 – 2304.

[4] Bradl, H. (2006) Energy foundations and other thermo active ground structures. *Geotechnique* 56 (2), 81 – 122.

[5] Loveridge, F. & Powrie, W. (2013) Temperature response functions (G-Functions) for Single Pile Heat Exchangers, *Energy*, 57, 554 – 564.

[6] Loveridge, F. & Powrie, W. (2013) Pile heat exchangers: thermal behaviour and interactions, *Proc ICE Geotechnical Engineering,* 166, (2), 178-196.

[7] Li, M. & Lai, A. C. K. (2012) New temperature response functions (G-functions) for pile and borehole ground heat exchangers based on composite-medium-line-source theory, Energy, 38, 255 – 263.

[8] Man, Y., Yang, H., Diao, N., Liu. & Fang, Z. (2010) A new model and analytical solutions for borehole and pile ground heat exchangers, *International Journal of Heat and Mass Transfer*, 53, 253-2601.

[9] Hellstrom, G. (1991) *Ground Heat Storage, Thermal Analysis of Duct Storage Systems, Theory*, Department of Mathematical Physics, University of Lund, Sweden.

[10] Lamarche, L. & Beauchamp, B. (2007) A new contribution to the finite line-source model for geothermal boreholes, *Energy & Buildings*, 39 (2), 188 – 198.

[11] Eskilson, P. (1987) Thermal Analysis of Heat Extraction Boreholes. Doctoral Thesis, University of Lund, Department of Mathematical Physics. Lund, Sweden.

[12] Ingersoll, L. R., Zobel, O. J. & Ingersoll, A. C. (1954) *Heat Conduction with Engineering and Geological Applications*. 3rd Edition, New York, McGraw-Hill.

[13] Bernier, M. (2001) Ground Coupled Heat Pump System Simulation, *ASHRAE Transactions*, 107 (1), 605-616.

[14] Loveridge, F. (2012) The thermal performance of foundation piles used as heat exchangers in ground energy systems, Doctoral Thesis, University of Southampton, Faculty of Engineering and the Environment, Southampton, UK.

[15] Loveridge, F. & Powrie, W. (2013) Performance of Piled Foundations Used as Heat Exchangers, *18th International Conference for Soil Mechanics and Geotechnical Engineering,* Paris, France, September 2-5, 2013.

[16] Hellström, G., Sanner, B., Klugescheid, M., Gonka, T. & Mårtensson, S. (1997) Experiences with the borehole heat exchanger software EED, *Proceedings of MEGASTOCK 97*, Sapporo, Japan, 247-252.

[17] Spitler, J.D. (2000) GLHEPRO -- A Design Tool For Commercial Building Ground Loop Heat Exchangers. *Proceedings of the Fourth International Heat Pumps in Cold Climates Conference, Aylmer, Québec*. August 17-18, 2000.

[18] Wood, C. J., Liu, H. & Riffat, S. B. (2010a) An investigation of the heat pump performance and ground temperature of a pile foundation heat exchanger system for a residential building, *Energy*, 35 (12), 3932-4940.

[19] Wood, C. J., Liu, H. & Riffat, S. B. (2010b) Comparison of a modeled and field tested piled ground heat exchanger system for a residential building and the simulated effect of assisted ground heat recharge, *International Journal of Low Carbon Technologies*, 5 (12), 137-143.

[20] Arup (2005) DTI Partners in Innovation 2002, Ground Storage of Building Heat Energy, Overview Report, O-02-ARUP3, May 2005. Available at: http://www.arup.com/_assets/_download/download352.pdf [downloaded 13/03/2013]

[21] Katsura, T., Nagano, K., Takeda, S. (2008) Method of calculation of the ground temperature for multiple ground heat exchangers, *Applied Thermal Engineering*, 28, 1995-2004.

[22] Katsura, T., Nagano, K., Narita, S., Taekda, S. & Nakamura, Y. (2009) Calculation algorithm of the temperatures for pipe arrangement of multiple ground heat exchangers, *Applied Thermal Engineering*, 29, 906-919.

[23] Hellstrom, G. (1989) *Duct Ground Heat Storage Model, Manual for Computer Code*. Department of Mathematical Physics, University of Lund, Sweden.

[24] Claesson, J. & Hellstrom, G. (1981) Model studies of duct storage systems, In: Millhone, J. P. & Willis, E. H. (eds.) *Proceedings of the International Conference on New Energy Conservation Technologies and their Commercialisation*, 6th – 10th August, 1981, Berlin, International Energy Agency.

[25] Hellstrom, G. (1983) Comparison between theoretical models and field experiments for ground heat systems, In: *Proceedings International Conference on Subsurface Heat Storage in Theory and Practice*, June 6 – 8, Stockholm, Volume 2, Swedish Council for Building Research.

[26] Pahud, D. (2007) *PILESIM2, Simulation Tool for Heating/Cooling Systems with Heat Exchanger Piles or Borehole Heat Exchangers*, User Manual, Scuola Universitaria Professionale della Svizzera Italiana, Lugano, Switzerland.

[27] Pahud, D., & Hubbuch, M. (2007b) *Mesures et optimisation de l'installation avec pieux energetiques du Dock Midfoeld de l'aeroport de Zurich*, Swiss Federal Office of Energy, June 2007.

[28] Markiewicz, R., 2010. Pers. Comm.

[29] Fan, R. Jiang, Y., Yao, Y. & Ma, Z. (2008) Theoretical study on the performance of an integrated ground source heat pump system in a whole year, *Energy*, 33, 1671 – 1679.

[30] Zanchini, E., Lazzari, S. & Priarone, A. (2012) Long-term performance of large borehole heat exchnager fields with unbalanced seasonal loads and groundwater flow, *Energy*, 38, 66 – 77.

[31] Teza, G., Galgaro, A. & De Carli, M. (2012) Long term performance of an irregular shaped borehole heat exchanger system: analysis of real pattern and regular grid approximation, *Geothermics*, 43, 45 – 56.

[32] de Paly, M., Hecht-Mendez, J., Beck, M., Blum, P., Zell, A. & Bayer, P. (2012) Optimization of energy extraction for closed shallow geothermal systems using linear programming, *Geothermics*, 43, 57 – 65.

[33] Beck, M., Bayer, P., de Paly, M., Hecht-Mendez, J. & Zell, A. (2013) Geometric arrangement and operation mode adjustment in low-enthalpy geothermal borehole fields for heating, *Energy*, 49, 434 – 443.